Atmospheric
Measurement
Techniques
Open Access

Discussions

A smog chamber comparison of a microfluidic derivatization measurement of gas-phase glyoxal and methylglyoxal with other analytical techniques

X. Pang[1,3], A. C. Lewis[2], A. Richard[2], M. T. Baeza-Romero[4], T. J. Adams[5], S. M. Ball[5], M. J. S. Daniels[5], I. C. A. Goodall[5], P. S. Monks[5], S. Peppe[6], M. Ródenas García[7], P. Sánchez[7], and A. Muñoz[6]

[1]Department of Chemistry, University of York, Heslington, York, YO10 5DD, UK
[2]National Centre for Atmospheric Science, University of York, Heslington, York, YO10 5DD, UK
[3]Key Laboratory for Aerosol-Cloud-Precipitation of China Meteorological Administration, Nanjing University of Information Science and Technology, Nanjing, 210044, China
[4]Escuela de Ingeniería Industrial de Toledo, Universidad de Castilla la Mancha, Toledo, 45071, Spain
[5]Department of Chemistry, University of Leicester, University Road, Leicester, LE1 7RH, UK
[6]School of Earth and Environment, University of Leeds, Woodhouse Lane, Leeds, LS2 9JT, UK
[7]Instituto Universitario Centro de Estudios Ambientales del Mediterráneo (CEAM-UMH), Spain

Discussion Paper | Discussion Paper | Discussion Paper | Discussion Paper |

AMTD

6, 5751–5794, 2013

A microfluidic measurement of glyoxal and methylglyoxal

X. Pang et al.

Title Page

Abstract | Introduction

Conclusions | References

Tables | Figures

◀ | ▶

◄ | ►

Back | Close

Full Screen / Esc

Printer-friendly Version

Interactive Discussion

A microfluidic measurement of glyoxal and methylglyoxal

X. Pang et al.

Title Page

Abstract	Introduction
Conclusions	References
Tables	Figures

 I◀ ▶I

◀ ▶

Back Close

Full Screen / Esc

Printer-friendly Version

Interactive Discussion

Abstract

A microfluidic lab-on-a-chip derivatization technique has been developed to measure part per billion volume (ppbV) mixing ratios of gaseous glyoxal (GLY) and methylglyoxal (MGLY), and the method compared with other techniques in a smog chamber experiment. The method uses o-(2,3,4,5,6-pentafluorobenzyl) hydroxylamine (PFBHA) as a derivatization reagent and a microfabricated planar glass micro-reactor comprising an inlet, gas and fluid splitting and combining channels, mixing junctions, and a heated capillary reaction microchannel. The enhanced phase contact area-to-volume ratio and the high heat transfer rate in the micro-reactor result in a fast and highly efficient derivatization reaction, generating an effluent stream ready for direct introduction to a gas chromatograph-mass spectrometer (GC-MS). A linear response for GLY was observed over a calibration range 0.7 to 400 ppbV, and for MGLY of 1.2 to 300 ppbV, when derivatized under optimal reaction conditions. The method detection limits (MDLs) were 80 pptV and 200 pptV for GLY and MGLY respectively, calculated as 3 times the standard deviation of the S/N of the blank sample chromatograms. These MDLs are below or close to typical concentrations in clean ambient air. The feasibility of the technique was assessed by applying the methodology under controlled conditions to quantify of α-dicarbonyls formed during the photo-oxidation of isoprene in a large scale outdoor atmospheric simulation chamber (EUPHORE). Good general agreement was seen between microfluidic measurements and Fourier Transform Infra Red (FTIR), Broad Band Cavity Enhanced Absorption Spectroscopy (BBCEAS) and a detailed photochemical chamber box modelling calculation for both GLY and MGLY. Less good agreement was found with Proton-Transfer Reaction Time-of-Flight Mass Spectrometry (PTR-ToF-MS) and Solid Phase Microextraction (SPME) derivatization methods for MGLY measurement.

1 Introduction

Glyoxal (GLY, CH(O)CHO) and methylglyoxal (MGLY, $CH_3C(O)CHO$) are the most prevalent α-dicarbonyls in the ambient atmosphere. They are found ubiquitously in urban, rural and remote ambient air owing to their wide variety of sources. Both α-dicarbonyls are generated by the photochemical oxidation of anthropogenic and biogenic volatile organic compounds (VOCs) (Henry et al., 2012). They are important primary ring opening products in the OH initiated oxidation of monoaromatic compounds in the presence of NO_X (NO and NO_2) (Calvert et al., 2002) and are photo-oxidation products from isoprene degradation as well as other biogenic VOCs (Calvert et al., 2000). Moreover, GLY and MGLY have attracted recent attention as potentially important contributors to global secondary organic aerosol (SOA) (Volkamer et al., 2009; Hallquist et al., 2009; Hoffmann et al., 1997), which can significantly impact climate, air quality and human health (Solomon, 2007; Mauderly and Chow, 2008). They are highly water-soluble and can form SOA through their uptake into the aqueous phase of an aerosol particle or cloud droplets, followed by aqueous-phase reactions that lead to the formation of low-volatility organosulphate/oligomeric products (De Haan et al., 2009; Fu et al., 2008; Loeffler et al., 2006). GLY was reported to account for up to 15 % of the mass of SOA in Mexico city (Volkamer et al., 2007).

However observations of α-dicarbonyls are rather limited, especially in rural and remote regions, where their mixing ratios are in the parts per trillion range, but can vary considerably depending on location. Low tens to hundreds of pptV concentrations (GLY: 15–1820 pptV and MGLY: 50–320 pptV) have been reported in rural, urban, and marine/open ocean environments (Lee et al., 1995; Munger et al., 1995; Spaulding et al., 2003; Fu et al., 2008; Huisman et al., 2008; Vrekoussis et al., 2009; Sinreich et al., 2010). Gaseous GLY concentrations have been observed up to 1.82 ppbV in Mexico City (Volkamer et al., 2005) and as high as 1.60 ppbV above a south-east Asia tropical rainforest (MacDonald et al., 2012). Globally, the majority of GLY (47 %) and MGLY (79 %) are produced by isoprene photo-oxidation (Fu et al., 2008), which is the

most abundant VOC emitted into the atmosphere, with an estimated annual emission from the biosphere of $500\,\mathrm{Tg\,yr^{-1}}$ of isoprene (Guenther et al., 1995). Other important sources of α-dicarbonyls include the oxidation of unsaturated hydrocarbons like acetylene (GLY only) (Fu et al., 2008), and alkenes (Calvert et al., 2000) (e.g. 2-methyl-3-buten-2-ol (Chan et al., 2009), methyl substituted ethenes (Volkamer et al., 2007) and, monoaromatics (Tuazon et al., 1984) (e.g. benzene (GLY only), toluene, xylene and 1,3,5-trimethylbenzene (MGLY only), Volkamer et al., 2007, 2005). MGLY is also formed from the oxidation of acetone (Fu et al., 2008), hydroxyacetone and various oxygenated alkenes (e.g. methylacrolein and methylvinylketone, Galloway et al., 2011) with GLY formed from glycolaldehyde, acrolein and crotonaldehyde, which are important components of biomass burning plumes (Magneron et al., 2005).

GLY and MGLY are reactive and have lifetimes of the order of a few hours during the daytime. Their atmospheric sinks are controlled primarily by photolysis, reaction with OH and heterogeneous processes (Volkamer et al., 2005; Fu et al., 2008). Therefore, both α-dicarbonyls have been used as tracers of local vs. regional photochemistry of biogenic and anthropogenic VOCs, since their short lifetimes inhibit their long-range transport (Henry et al., 2012; Volkamer et al., 2007). Additionally, the photolysis of GLY and MGLY can be a significant source of tropospheric HO_x ($HO + HO_2$) and their reactions with OH can contribute to the tropospheric burden of ozone (Henry et al., 2012). Since α-dicarbonyls form as part of, and contribute to, the complex intermediary atmospheric chemistry of both ozone and SOA formation, they are attractive species to measure in order to test our fundamental chemical understanding, under a variety of atmospheric regimes, through mechanism evaluation of chemistry incorporated into predictive policy and scientific models (e.g. the Master Chemical Mechanism) (Jenkin et al., 2003).

Despite the importance of α-dicarbonyls in gas-phase atmospheric photochemistry and SOA formation, cheap and simple techniques for their rapid and sensitive in situ atmospheric measurement have not been readily available. In recent years several different optical/spectroscopic approaches have been proposed for atmospheric measure-

A microfluidic measurement of glyoxal and methylglyoxal

X. Pang et al.

Back | Close

Full Screen / Esc

Printer-friendly Version

Interactive Discussion

ment of α-dicarbonyls including Differential Optical Absorption Spectroscopy (DOAS) (Volkamer et al., 2005; MacDonald et al., 2012), Broad Band Cavity Enhanced Absorption Spectroscopy (BBCEAS) (Thalman and Volkamer, 2010; Washenfelder et al., 2008), Laser-Induced Phosphorescence (LIP) Spectrometry (Henry et al., 2012), and
5 Fourier Transform InfraRed (FTIR) absorption spectroscopy (Connelly et al., 2012; Profeta et al., 2011). DOAS is a well-established technique used to identify trace gases by means of their individual differential (i.e., narrow band) absorption structures. Volkamer et al. demonstrated long-path differential optical absorption spectroscopy (LP-DOAS) in Mexico City to detect GLY with a detection limit of 150 pptV using an atmospheric path
10 length of 4420 m and integration times between 2 to 15 min (Volkamer et al., 2005). GLY above a south-east Asian tropical rainforest was measured by LP-DOAS and multi-axis (MAX) DOAS with a maximum mixing ratio of 1.6 ppbV observed (MacDonald et al., 2012). Broadband methods based on making absorption measurements on gas samples within high finesse optical cavities are a promising, emerging detection technique
15 for many atmospheric trace gases with broad, structured absorptions in the visible and ultraviolet spectral regions (Thalman and Volkamer, 2010; Washenfelder et al., 2008, 2011; Langridge et al., 2008). Cavity Enhanced Differential Optical Absorption Spectroscopy (CE-DOAS) has been shown to be capable of sensitive, in situ single point measurements of GLY with method detection limit (MDL) as low as 28.5 pptV with one
20 minute averaging and MGLY with MDL of 170 pptV with one minute averaging (Thalman and Volkamer, 2010). A similar spectroscopic method, Broad Band Cavity Enhanced Absorption Spectroscopy (BBCEAS) can achieve a MDL for GLY of 87 pptV with one minute averaging (Washenfelder et al., 2008). Huisman et al. recently demonstrated a Laser-Induced Phosphorescence (LIP) technique for GLY measurement with a MDL
25 of 18 pptV in one minute and high time resolution (up to 3 Hz) (Huisman et al., 2008, 2011). The LIP technique has recently been improved to enable the simultaneous measurement of GLY and MGLY with MDLs of 11 pptV in 5 min for GLY and 243 pptV for MGLY (Henry et al., 2012). The LIP technique is a sensitive, in situ technique but the light source is expensive and complex.

In fact, many of the optical methods reviewed above require some highly specialist, or high maintenance equipment, or potentially require a dedicated instrument for the measurement of individual α-dicarbonyls. More commonly available, FTIR is a well-established means to measure atmospheric gases and has been proven particularly useful as a benchmark standard for inter-comparison studies in polluted urban atmospheres (Finlayson-Pitts and Pitts Jr., 1999). However, one drawback in the application of FTIR to ambient air is that water, CO_2 and CH_4, which are all present in significant concentrations and absorb strongly in certain regions of the spectrum, limit the spectral regions accessible for ambient air measurements (Finlayson-Pitts and Pitts Jr., 1999).

Global GLY measurements have recently become available from satellites. Several space-borne imaging UV-VIS-near IR spectrometers have been used to observe GLY from space and retrieve global total column GLY datasets, including the SCanning Imaging Absorption SpectroMeter for Atmospheric CartograpHY (SCIAMACHY), Global Ozone Monitoring Experiment (GOME) and GOME-2 instruments (Vrekoussis et al., 2009, 2010; Wittrock et al., 2006). Importantly, however, such satellites measurements, based on complex retrievals, require extensive validation by in situ measurements on the ground, ideally over a wide range of spatial and temporal scales. Satellite observations are good for providing a global picture of distribution but they may only typically produce one pixel of information to cover a whole city, which does not provide enough information if, for example, researchers want to use GLY and MGLY as a tracer for fast photochemistry. Therefore, the complementarity of detailed in situ measurements and satellite observation is required.

A common and versatile method for GLY and MGLY measurement uses the principle of chemical derivatization with a derivatization reagent, such as *o*-(2,3,4,5,6-pentafluorobenzyl)hydroxylamine (PFBHA) (Ho and Yu, 2002; Temime et al., 2007), pentafluorophenylhydrazine (PFPH) (Pang and Lewis, 2011; Pang et al., 2011; Ho and Yu, 2004), and 2,4-dinitrophenylhydrazine (DNPH) (Ho and Yu, 2004; Lee et al., 1998) with subsequent analysis using bench-top GC-MS or High Performance Liquid Chromatography with ultraviolet detection (HPLC-UV). Derivatization approaches have

been used widely in the measurement of α-dicarbonyl species since they allow trace-level measurements to be made with commonly available and reasonably low cost GC-MS technology. An advantage of this type of approach is that it yields information on the complete ensemble of carbonyl compounds from HCHO to high molecular weight OVOCs.

The sample preparation methodology in general consists of trapping gaseous GLY and MGLY on solid absorbents or filters coated with the derivatization reagent or entraining GLY and MGLY into solution using a bubbler or impinger. The resulting derivatives can subsequently be desorbed by an appropriate solvent, concentrated and then separated and detected by GC-MS or HPLC-UV. Such methods have acceptable sensitivity, good reproducibility and the considerable advantage of being able to quantify multiple compounds simultaneously. Although derivatization methods are fully applicable for the measurement of GLY and MGLY, the drawbacks are long sampling times, typically 1–2 h, with a lengthy and complicated lab procedure of derivatization and solvent extraction/evaporation following sampling of ambient air. Sampling times can be reduced to 10 min or less using the method of PFBHA on-fibre derivatization with Solid Phase Microextraction (SPME). However, the detection range of the SPME technique is limited to higher concentrations compared with other derivatization techniques owing to only small quantities of derivatization reagent absorbing on the fibre (Gomez Alvarez et al., 2009). Furthermore, the preparation processes for PFBHA-coated SPME are complicated and labour intensive. This creates a considerable experimental overhead if the aim is to sample continuously over an extended time period. It is clear that substantial benefits may be gained from the employment of a methodology which can utilise the universality of a GC-MS method whilst eliminating the bench chemistry required for sample preparation. The key to making major improvements in GLY and MGLY measurements may therefore lie in near-automated sample preparation.

In this work, a rapid, simple and sensitive microfluidic derivatization approach for GLY and MGLY analysis has been developed using accelerated and highly efficient derivatization reactions between α-dicarbonyls and a derivatization reagent inside a micro-

A microfluidic measurement of glyoxal and methylglyoxal

X. Pang et al.

Title Page

Abstract | Introduction

Conclusions | References

Tables | Figures

◄ | ►

◄ | ►

Back | Close

Full Screen / Esc

Printer-friendly Version

Interactive Discussion

reactor. The micro-reactor provided a zone for gas sample mixing, chemical reaction and pre-concentration, essentially replacing three independent offline preparative steps: hence we use the "lab-on-a-chip" moniker for the methodology. This methodology for GLY and MGLY builds on our previous reported techniques used to measure gas phase formaldehyde (Pang and Lewis, 2012). The micro-reactor comprises a planar Pyrex glass microfluidic chip containing a long circular cross section micro-channel, providing a capillary volume for the reaction to occur in. The microfluidic technique realises a near real-time analysis based on the rapid derivatization reaction occurring simultaneously with air sampling at high chip temperatures, and without any post-derivatization treatment necessary on the samples. Combining the micro-reactor with the auto-sampler of a commercial GC-MS allows for continuous sampling and analysis with a time resolution of around 30 min or less.

The performance of the microfluidic derivatization technique is evaluated in this paper through simultaneous measurement of gaseous GLY and MGLY in various experiments performed at the European Photoreactor (EUPHORE), a highly instrumented, large-scale outdoor atmospheric simulation chamber located in Valencia, Spain. The microfluidic derivatization technique was compared with FTIR, BBCEAS, PTR-ToF-MS, and SPME observations as well as with a detailed model simulation of the temporal evolution of GLY and MGLY formed during the photo-oxidation of isoprene.

2 Experimental

2.1 Micro-reactor layout and analytical system

The layout of the micro-reactor is shown in Fig. 1a. The microfluidic chip was installed with a chip holder and chip header to allow quick connection to 1/16th inch external diameter tubing through its three inlets and one outlet (Fig. 1a). The detailed description of the micro-reactor can be seen on our previous study (Pang and Lewis, 2012) In this study the micro-reactor integrates three key functions: (1) a gas and liquid mixer and

A microfluidic measurement of glyoxal and methylglyoxal

X. Pang et al.

Title Page

Abstract | Introduction

Conclusions | References

Tables | Figures

◀ | ▶

◀ | ▶

Back | Close

Full Screen / Esc

Printer-friendly Version

Interactive Discussion

reactor, (2) reagent heating, and (3) sample pre-concentration. Gaseous mixtures containing GLY and MGLY are drawn into the micro-reactor through inlet 2 and inlet 3 by the clean air pump. The PFBHA derivatization solution was introduced into the micro-reactor simultaneously through inlet 1 by a peristaltic pump (Watson Marlow 205S, UK) (see Fig. 1b). The micro-reactor was fixed securely on the surface of a hotplate head for direct heating. GLY and MGLY in the gas stream reacted with PFBHA with high efficiency in the micro-channel through diffusion into the derivatization solution which formed a laminar layer on the channel walls, analogous to a capillary chromatography stationary phase (Pang and Lewis, 2012). A stainless metal coil (50 cm in length) was connected to the outlet of the micro-reactor, and placed in an ice-salt bath with a temperature of 0 °C. The reaction solution eluting from the stainless coil was collected directly into a sample vial within the auto-sampler of the GC-MS (Fig. 1b).

2.2 Materials and apparatus

All chemicals (unless otherwise stated) were purchased from Sigma-Aldrich Company. Solvents including acetonitrile, methanol, ethanol, ethyl acetate, 2-propanol (HPLC grade) were purchased from Fisher (UK). The derivatization reagent *o*-(2,3,4,5,6-pentafluorobenzyl) hydroxylamine (PFBHA) (99 %), was used directly in this study without any further purification. The sample gases matrix including GLY, MGLY was pumped into the micro-reactor using a clean KNF diaphragm gas pump (PM20994-022, Neuberger, Germany). Flow rate of sample gas was controlled by a mass flow controller (Model GFC17, Aalborg, USA), itself calibrated by a gas flow meter (Alicat Scientific, USA). Flow of the derivatization solution was generated and controlled by a peristaltic pump, varying from 20–120 μL min^{-1}. A magnetic stirrer hotplate (RH Basic 2 IKA-MAG, UK) with a contact thermometer was used to heat the microchip directly. Separation and detection of the PFBHA derivatives of GLY and MGLY were performed on a GC-MS system incorporating a Perkin Elmer (USA) Auto system XLGC and a Turbo Mass (USA) quardrupole MS equipped with a DB5 column (60 m × 0.25 mm × 1.0 μm, length × internal diameter × film thickness). GC conditions were as follows: the GC

oven temperature was initially set at 80 °C for two minutes, programmatically ramped to 300 °C with a temperature ramp of 8 °C min^{-1} and then held at 300 °C for 1.5 min. The solvent delay was set at 10 min to avoid possible damage to the MS detector. The GC injection mode was set as splitless. The temperatures of the GC inlet and GC-MS transfer line were kept at 250 °C. The mass spectrometer was operated in scan mode with a mass range of 100–500 Da to identify the most abundant ions. The selected ion chromatograms of the most abundant ion ($[C_6F_5CH_2]^+$) with $m/z = 181$ Da, which is a fragment of the PFBHA molecule, were used to quantify the concentration of derivatives in solution.

2.3 Description of EUPHORE chamber and instrumentation

All experiments were performed in the European Photo-Reactor (EUPHORE), located in Valencia, Spain during the period of 28 June to 2 August 2012. EUPHORE consists of two hemispherical FEP (fluorine ethene propene) chambers mounted on aluminium floor panels. The FEP foil is highly transparent even to short-wavelength sunlight. The chamber used in the present study has a volume of 200 m^3 and is protected by retractable hemispherical shutters when it is not in use or the presence of sunlight is not required. The chamber is operated at ambient temperature and approximately atmospheric pressure using purified air, while two large fans provide homogeneous mixing of the chamber contents.

The chamber is equipped with a multi-pass White-Cell mirror system for long path in situ monitoring of gaseous reactants and products by FTIR spectrometry. The spectrometer (NICOLET 550, MCT/B-detector) is coupled to the long-path multi-reflection cell for detection in the IR spectral range (400–4000 cm^{-1}). The gold-coated mirrors of the cell allow for a total path length of 616 m. Spectra are collected with 1 cm^{-1} resolution by averaging 280 scans, resulting in a sampling time of 5 min per spectrum. Concentrations of GLY and MGLY in the chamber during the experiments were determined with improved analysis software developed at CEAM using calibrated reference spectra collected a priori (Ródenas, 2008). GLY and MGLY were monitored in the

aldehydic C-H band, within the spectral region of 2750–2900 cm^{-1} for GLY and 2750–2920 cm^{-1} for MGLY. For the calibration of gases measured by FTIR, GLY was injected into the chamber with a syringe in repeated trials while MGLY was cross-calibrated against DOAS. The linear range of FTIR measurement for GLY is 2.5 ppbV–3.5 ppmV with MDL 2.5 ppbV and for MGLY is 2.7 ppbV–4.2 ppmV with MDL 2.7 ppbV. The accuracy is estimated to be 8 % for GLY measurement and 15 % for MGLY measurement for FTIR in this study.

A custom-built Broadband Cavity Enhanced Absorption Spectroscopy (BBCEAS) instrument was also employed to monitor GLY and MGLY. The BBCEAS instrument has been developed for highly sensitive and target-selective in situ trace gas measurements building on previous instrument development work for quantifying atmospheric NO_2 and NO_3 (Langridge et al., 2008). A blue light emitting diode (LED) is employed as the light source, enabling simultaneous measurements of GLY, MGLY and NO_2 to be made using these molecules' distinctive spectral signatures in the wavelength range 430–488 nm. In the configuration deployed at the EUPHORE chamber, the BBCEAS instrument has a 3σ method detection limit (MDL) of 75 pptV for GLY and 1.05 ppbV for MGLY in 10 s against a background containing no other absorption signals. The accuracy of the BBCEAS measurements is determined by two main considerations: (i) uncertainties in the reference absorption cross sections used to fit the differential spectral structure in the BBCEAS spectra to retrieve the target absorber concentrations, and (ii) uncertainties in determining the reflectivity of the cavity mirrors (i.e. the effective path length of the BBCEAS absorption measurement) and the proportion of the cavity occupied by the gas sample (the cavity mirrors are purged with synthetic air to prevent contamination). The overall accuracies of the BBCEAS measurements are estimated to be 7 % for GLY and 10 % for MGLY.

Solid Phase Microextraction (SPME) was also used to determine GLY and MGLY through PFBHA on-fibre derivatization. Detailed descriptions of this methodology can be found in the previously published literature (Gomez Alvarez et al., 2009). In short, the fibres, which were conditioned in the injector of a GC at 250 °C, were loaded with

PFBHA derivatization reagent through the headspace of a 4 mL opaque amber vial containing a 17 mg mL^{-1} solution of PFBHA in water. Gas samples were extracted from the EUPHORE chamber by inserting the SPME holder into a built-in adapter in one of the chamber's flanges. Sampling times ranged from 2 to 5 min depending on the α-dicarbonyl concentrations. GLY and MGLY were then quantified using a 6890 HP Gas Chromatograph with a flame ionization detector (GC-FID) through the formation of the corresponding oxime by reaction of GLY or MGLY with PFBHA on the fibres. The linear range for GLY is 1–130 ppbV and for MGLY is 1–80 ppbV. MDL is 0.1 ppbV for GLY and 0.15 ppbV for MGLY. The accuracies are 30 % for both GLY and MGLY measurements by the SPME derivatization technique.

A PTR-ToF-MS instrument (Series I, Kore, UK) was also used to detect the gaseous MGLY. The PTR-ToF-MS technique is based on the chemical ionization of trace VOCs present in atmospheric samples by proton transfer reactions with the hydronium reagent ion (H$_3$O$^+$). The product is a protonated molecular ion (VOC-H)$^+$ for each VOC which is then selected and quantified by time-of-flight mass spectrometry (Blake et al., 2009). The PTR-ToF-MS method is also applicable to oxygenated VOCs such as GLY and MGLY. However, one drawback to PTR-MS, common to mass spectrometric techniques, is isobaric interference between VOC species being sampled. GLY is isobaric with propanal and acetone and as a result GLY cannot be exactly quantified by PTR-ToF-MS in this study. Only MGLY was measured based on the $m/z = 73$ Da signal for MGLY-H$^+$. The linear range for MGLY is 1.5 ppbV–172 ppbV by PTR-ToF-MS measurement with a MDL (3σ) of 1.5 ppbV. The instrumental error on the MGLY measurement is 1.0 ppbV.

2.4 Preparing gaseous GLY and MGLY

Pure GLY monomer was prepared from the solid trimer-dihydrate (95 %) using the same method as described in the literature (Feierabend et al., 2009) MGLY is available commercially as 40 % aqueous solutions wherein it exists primarily in its monohydrate and dihydrate forms. To obtain the unpolymerized and water-free form, the following

procedures were conducted as described in the previous study (Gurnick et al., 1981). Flasks containing pure and unpolymerized GLY or MGLY were stored in liquid nitrogen prior to experimental use.

Pure GLY or MGLY was introduced into the EUPHORE chamber by passing a small flow of nitrogen through a cold-trap whilst allowing the trap to warm gently. After each addition, the chamber's contents were homogenously mixed by the fans and stabilized for five minutes. Therefore, a stable GLY and MGLY gaseous mixture inside the chamber was obtained. Chamber measurements were taken for a period of 30 min before dilution down to a lower concentration by adding clean air, allowing the chamber contents to mix thoroughly and measuring for a period of 30 min repeatedly until GLY and MGLY concentrations were below the detection limits. The detailed temporal variations of α-dicarbonyl concentrations are shown in Fig. 2a. Therefore, the downward steps provide a series of gas phase calibrations of GLY and MGLY over a representative range of concentrations generated inside the EUPHORE chamber during experiments performed to investigate the photo-chemical oxidation of VOCs. The different chamber amounts of GLY and MGLY were used to test the instrument response and linearity, and assigned absolute mixing ratio values using the co-measurements by FTIR (ranging from 2.5 ppbV to 405 ppbV for GLY and from 5.4 ppbV to 227 ppbV for MGLY) and BBCEAS (ranging from 1.0 ppbV for GLY and 0.7 ppbV for MGLY). Given their similar performances in previous GLY and MGLY measurement experiments (Fig. 2b and c), these two techniques were chosen as the reference instruments to evaluate the performance of the microfluidic derivatization technique.

2.5 Preparing standard solutions of PFBHA-dicarbonyl derivatives

A set of known concentrations of the PFBHA-dicarbonyl derivatives were prepared in acetonitrile by mixing the α-dicarbonyls with a PFBHA solution whose concentration is five times higher than the highest concentration of α-dicarbonyls. Six standards of individual α-dicarbonyls were prepared ranging from 5.6 to 33.6 µmol L^{-1} (5.6, 11.2, 16.8, 22.4, 28.0 and 33.6 µmol L^{-1}). They are equal to the quantities of α-dicarbonyl deriva-

tives formed by 6.7, 13.4, 20.1, 26.8, 33.5, and 40.2 ppbV of gaseous α-dicarbonyls in the chamber conditions (30 °C at 1 atm) reacting with PFBHA, assuming 100 % reaction efficiencies under the optimal micro-reactor conditions shown in Table 1, with a solution enriching ratio of 2.77 (Pang and Lewis, 2012). We consider that such a liquid based calibration would present a feasible approach for any future field instrument.

2.6 Accuracy and precision

Standard α-dicarbonyl mixtures of gases of three different concentrations were prepared in the chamber and used to check the method accuracy and precision. The accuracy of the method was evaluated by the relative error which is expressed as [(observed concentration – absolute concentration)/absolute concentration] × 100 %. Five parallel samples for each concentration were collected continuously. The absolute concentrations of GLY and MGLY are provided by the BBCEAS due to its better accuracy over FTIR for this species. The observed concentrations were measured by the microfluidic derivatization technique under the optimal experimental conditions as shown in Table 1 using a peak height calculation based on the calibration curves. Ignoring the uncertainties introduced by the FTIR and BBCEAS measurement, the microfluidic derivatization has two main sources of error: (i) the experimental uncertainties of microfluidic derivatization technique, assessed using parallel samples under the identical experimental conditions, (ii) the instrumental uncertainties of the GC-MS response, assessed here by multiple injections of the same sample under the same instrumental conditions. The precision of the new analytical method is controlled by two elements, the reproducibility of microfluidic reactor and of the GC-MS instrument. The precision of the microfluidic derivatization technique was determined by the replicate analyses ($n = 5$) of standard α-dicarbonyl gases at three different concentrations under the same experimental conditions. The precision of the GC-MS instrument to the same sample was calculated by repeated measurements ($n = 5$) under the same GC-MS instrumental conditions. The precision was expressed as the relative standard deviation (RSD) = [(standard deviation of observed concentration)/(average of observed concentration)] × 100 %.

2.7 EUPHORE isoprene photo-oxidation experiment

The microfluidic derivatization technique was employed through the whole campaign to determine the gaseous GLY and MGLY in the EUPHORE chamber. To illustrate the microfluidic derivatization technique capability, its performance on 25 July 2012 is chosen. For this particular experiment, isoprene photo-oxidation was carried out under relatively low NO_X conditions (initial VOC/NO_X ratio of about 7). 226 ppbV of isoprene was prepared by injecting 170 µL of isoprene (liquid phase) into the chamber by a heated air flow. Sulfur hexafluoride (SF_6) was also added in order to monitor the chamber dilution (using FTIR). HONO was subsequently continuously added into the chamber throughout the experiment so that a steady state of 5–8 ppbV of HONO was achieved (monitored by a Long Path Absorption Photometer (LOPAP) and FTIR) (Heland et al., 2001). This experiment was designed so that GLY and MGLY formation could be monitored throughout the entire chemical evolution of the isoprene photo-oxidation system (i.e. their primary formation from the initial OH reaction, secondary formation from reactions of methacrolein and methyl vinyl ketone products, and later-stage formation from glycolaldehyde and hydroxyacetone products (Calvert et al., 2000). After the gases in the chamber were mixed by the fans and stabilized for 5 min, the retractable half-spherical housing was opened exposing the chamber to solar radiation, photolysing HONO to produce OH radicals and thus initiating the photoxidation of isoprene. The chamber was closed when the formation of ozone had reached a maximum (after about 400 min). A comprehensive suite of instrumentation measuring gas and aerosol phase composition was available including those capable of sensitively monitoring the formation of GLY and MGLY (i.e. FTIR, BBCEAS, PTR-ToF-MS, and SPME). A gas sample was collected every 30 min from the chamber to measure the GLY and MGLY yields from isoprene photo-oxidation using the microfluidic derivatization technique.

The composition and evolution of the gas phase components of the isoprene photo-oxidation chamber system was also simulated using a chamber optimised photochemical box model incorporating the comprehensive isoprene photo-oxidation scheme ex-

tracted from the Master Chemical Mechanism (MCMv3.2) (Jenkin et al., 2003). The isoprene mechanism employed (along with an appropriate inorganic reaction scheme) contains 456 species and 1476 reactions. The box model used in this study also includes a series of "chamber specific" auxiliary reactions adapted from Bloss et al.
5   (2005) in order to take into account the background reactivity of the chamber walls (Rickard et al., 2010).

3   Results and discussions

The solvent, PFBHA concentration, microchip temperature, flow rates of gas and solution and reaction time can all affect the reaction efficiency and reproducibility of the
10 derivatization reaction and, therefore, an optimization of the parameters is required to achieve the highest efficiency of derivatization from each micro-preparative system. At the same time, in order to achieve a good separation, chromatographic conditions were optimized to the values described in Sect. 2.2. We have described previously the optimisation process and parameters for formaldehyde measurement (Pang and Lewis,
15 2012) and have undertaken a similar optimisation here.

The reaction between GLY/MGLY and PFBHA to form the corresponding pentafluorobenzyl oximes is a two-step process, as illustrated in Fig. 3. In the first step of the reaction, the PFBHA reacts with the α-dicarbonyl through nucleophilic attack to form an amino alcohol. The second step is dehydration of the amino alcohol, which leads to
20 formation of an oxime (Spaulding et al., 2002; Ho and Yu, 2002). When GLY and MGLY which contain two carbonyl groups are derivatized, two isomers are formed for GLY and four isomers (ZE, ZZ, EZ, EE isomers) are potentially formed for MGLY. However in practice, as seen in the GC chromatograms (Fig. 4a), only two of the four MGLY isomers are formed in significant concentrations. The retention times of one GLY deriva-
25 tive and one of the observed MGLY derivatives are so close that their peaks overlap and therefore cannot be resolved sufficiently using the current instrument. This phenomenon has been previously reported in published studies on derivatization of GLY

A microfluidic measurement of glyoxal and methylglyoxal

X. Pang et al.

and MGLY (Yu et al., 1995). Therefore only the GLY derivative with retention time of 26.4 min and MGLY derivative with retention time of 27.0 min were used to calculate the concentration of each α-dicarbonyl. The MS spectra of the two isolated peaks demonstrate that the two carbonyl groups of each α-dicarbonyl have both been derivatized with a molecular ion peaks of $m/z = 448$ Da for the GLY derivative and $m/z = 462$ Da for the MGLY derivative (Fig. 4b and c). The ion with m/z 181 Da is identified as the most abundant fragment ion for the two derivatives (Fig. 4b and c). Therefore, the selected ion chromatograms of the most abundant ion, $m/z = 181$ Da, previously shown to be a convenient indicator of the presence of carbonyl compounds (Yu et al., 1995), was used to quantify the concentration of derivatives.

3.1 Solvent selection for PFBHA

PFBHA is a water-soluble derivatization reagent for carbonyl-containing compounds. However, water is not a suitable solvent in this study since aqueous solutions cannot be easily injected directly into the capillary GC column. Instead, several organic solvents, including acetonitrile, ethanol, ethyl acetate, methanol, and 2-propanol were tested as the carrier solvent and their influences on the measurement were studied. Traces of some carbonyl compounds including formaldehyde, acetaldehyde, butyraldehyde were found in several PFBHA solvent combinations such as ethanol, ethyl acetate, methanol, and 2-propanol, which can potentially interfere with the PFBHA derivatization reactions of target carbonyl products such as formaldehyde, acetaldehyde, acetone, etc. formed in the chamber experiments (e.g. isoprene photo-oxidation).

Acetonitrile was not found to contain contaminant carbonyl compounds which produced derivative peaks in the GC chromatograph of PFBHA solutions. Therefore, acetonitrile was chosen as the optimal solvent to prepare the derivatization solution in this study.

3.2 Influence of PFBHA concentration

Increasing the liquid phase PFBHA concentration from $1.0 \times 10^{-4}\,\mathrm{mol\,L^{-1}}$ to $6.0 \times 10^{-4}\,\mathrm{mol\,L^{-1}}$ (whilst the GLY and MGLY concentrations were held constant at 50 ppbV) was found to improve the α-dicarbonyl-PFBHA derivatization yield. Positive relationships existed between the α-dicarbonyl derivative-oxime response and the PFBHA concentration for both GLY and MGLY (Fig. 5a). In a $1.0 \times 10^{-4}\,\mathrm{mol\,L^{-1}}$ PFBHA reaction solution, the signal responses (peak heights) of α-dicarbonyl derivatives are equal to 25 % of those of α-dicarbonyl derivatives in $6.0 \times 10^{-4}\,\mathrm{mol\,L^{-1}}$ PFBHA reaction solution. Since $6.0 \times 10^{-4}\,\mathrm{mol\,L^{-1}}$ is close to the saturated solubility of PFBHA in acetonitrile, this was the maximum PFBHA concentration tested. According to the derivatization mechanism there is reaction equilibrium between PFBHA and the α-dicarbonyl (R1) with the formation of an oxime derivative (PFBHA oxime):

$$2\,\mathrm{PFBHA} + \mathrm{Dicarbonyl} \overset{K}{\Leftrightarrow} \mathrm{PFBHA\ oxime} \tag{R1}$$
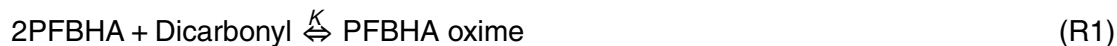
The equilibrium constant is expressed as Eq. (1)

$$K = \frac{[\mathrm{PFBHA\ oxime}]}{[\mathrm{Dicarbonyl}] \cdot [\mathrm{PFBHA}]^2} \tag{1}$$

Since the α-dicarbonyl concentrations are stable in solution under identical reaction conditions including the mixing ratio of α-dicarbonyl standard gases, Eq. (1) can be rearranged into the following Eq. (2):

$$[\mathrm{PFBHA\ oxime}] = K'[\mathrm{PFBHA}]^2 \tag{2}$$

According to Eq. (2) more PFBHA oxime will be produced when using a higher concentration of PFBHA reagent, which forces the equilibrium of reaction R1 heavily in favour of the oxime formation. Temime et al. also found that the higher molar ratio of PFBHA to carbonyls significantly promoted the derivative yields compared with lower ratio (Temime et al., 2007).

3.3 Optimization of reaction temperature and storage time

To the best of our knowledge, the influence of temperature on derivative yields has not previously been studied for the derivatization of α-dicarbonyls. Although temperature was reported to affect the efficiency of the derivatization reaction by the US EPA, no fur-
ther information was provided (Munch et al., 1998). In this study the derivative relative signal responses of GLY and MGLY were found to increase from about 40 % at 20 °C to 96 % at 50 °C as illustrated in Fig. 5b, which implies a higher reaction temperature is favourable to derivative yield. The reaction temperature of the micro-reactor was con-trolled by a hot plate. The micro-reactor can be heated directly to an elevated temper-
ature due to its planar shape, unlike more commonly used bubblers and impingers that are often used for stripping and derivitising reactions. Temperature affects the derivati-zation reaction in the microchannel via three processes: (1) the reaction rate between α-dicarbonyl and PFBHA, (2) the PFBHA and α-dicarbonyl partitioning between the gas and the liquid phases, (3) the partitioning of the PFBHA-α-dicarbonyl derivatives
between the liquid and the gas phases. For GLY, MGLY and PFBHA, increasing the temperature will accelerate the reaction rates between α-dicarbonyls and PFBHA re-sulting in more derivative formation in solution (Destaillats and Charles, 2002; Betterton and Hoffmann, 1988). It should be noted that too high a temperature leads to rapid sol-vent evaporation. Since the same GC-MS peak height was obtained at 50 °C, 60 °C and
80 °C, as shown in Fig. 5b, the optimal reaction temperature in this study was chosen as 60 °C.

Previous studies have found storage time to be an important factor in influencing the derivative yields. PFBHA derivative yields were reported to increase significantly after a storage period from one hour to several days depending on the species of car-
bonyl compound in previous studies (Ho and Yu, 2002; Temime et al., 2007). In this study the residence time of the gaseous carbonyls in the micro-channel is on the or-der of a few seconds. The derivatization reaction begins instantaneously but is not necessarily completed within the micro-channel and a solution storage time of ten min-

utes was still needed to allow the derivatization reaction to complete. In this study the peak heights of derivatives in the GC-MS chromatogram reached their maximum and remain relatively constant after around fifteen minutes (Fig. 5c). The longer storage time was found to have no significant effect on the GC-MS signal responses of GLY and MGLY derivatives even after 24 h storage, which is different from observations previously reported (Ho and Yu, 2002). Since the PFBHA derivatization process is effectively a nucleophilic addition reaction the simple steric structures and electron configurations of GLY and MGLY are favourable to the faster reaction rate (Temime et al., 2007; Reisen et al., 2003). The control parameters afforded by the combination of micro-reactor length and peristaltic flow rate means that the derivatization process is considered sufficiently fast that it can be used for near real-time measurement of α-dicarbonyls with the micro-reactor effluent passed directly for in-situ GC-MS analysis. Such an approach circumvents the problems associated with slow storage reactions and long-term degradation of derivative samples in solution.

3.4 Optimization of flows of gas and solution

A key function of the micro-reactor is to efficiently mix the gas flow containing the target α-dicarbonyls with the PFBHA solution. If the flow rate of the test gas is too high, the α-dicarbonyls do not have chance to dissolve in the wall liquid film and react causing the derivatization efficiency to decrease. The overall derivatization efficiency was influenced strongly by the mixing at the channel junction and downstream in the capillary region. The detailed discussion on effect of flow rates of gas and solution can be seen for HCHO in our previous study (Pang and Lewis, 2012).

Flow rates of the sample gas were varied from 100 to 600 mL min^{-1} and evaluated for peak height with the derivatization solution (5.0×10^{-4} mol L^{-1}) flow set at a constant 40 µL min^{-1} and the temperature of micro-reactor at 60 °C for both α-dicarbonyls with their concentrations of 50 ppbV. At lower flow rates (between 0 and 300 mL^{-1}) a stoichiometric increase in peak area is seen as the gas flow rate increases. Above this point, peak areas then increase more slowly, likely due to insufficient mixing and

reaction time in the microchip. Such high flow rates are therefore not appropriate to use for these compounds. It should be noted that too high a gas flow rate can also lead to excessive rapid solvent evaporation. In this study the optimal flow of α-dicarbonyl in gas was chosen as $200\,\mathrm{mL\,min^{-1}}$. Five flow rates of derivatization solution ($5.0 \times 10^{-4}\,\mathrm{mol\,L^{-1}}$) varying from 20 to $120\,\mathrm{\mu L\,min^{-1}}$ were assessed with the test gas flow kept at a constant $300\,\mathrm{mL\,min^{-1}}$ (all other conditions the same as Fig. 5d). Peak heights diminish as the liquid flow rate increases – a value of around 30–$40\,\mathrm{\mu L\,min^{-1}}$ gave good peak heights whilst retaining sufficient workable volumes of solution in the reactor for subsequent handling by GC-MS (Fig. 5e). The optimal flow rate of PFBHA derivatization solutions was chosen as $40\,\mathrm{\mu L\,min^{-1}}$ for both GLY and MGLY detection. Based on the above approaches, the optimal conditions of the micro-reactor for measurement of gas phase α-dicarbonyls are shown in Table 1.

3.5 Method calibration

The method calibration curves for the microfluidic derivatization technique were established based on measuring a series of GLY and MGLY gas mixtures of different concentration prepared in the EUPHORE chamber. The GLY and MGLY standard gas mixtures in the chamber were simultaneously determined by FTIR and BBCEAS techniques. Although the α-dicarbonyl concentrations can be calculated based on the known amount of GLY and MGLY injected into the chamber, their actual concentrations were checked by the measurements of FTIR and BBCEAS in order to construct calibration curves for the microfluidic derivatization technique which would also account for any wall losses of GLY and/or MGLY in the chamber or losses in the injection tube.

In practice the FTIR and BBCEAS instruments showed good agreement for the measurement of GLY and MGLY when mixing ratios were above 5 ppbV and 2 ppbV, respectively (Fig. 2a), though there is some evidence of divergence at the lowest mixing ratios. Two versions of the calibration equations are obtained according to the two optical techniques employed as shown in Fig. 6. One version (Fig. 6a) is based on the absolute GLY and MGLY concentrations provided by FTIR and the other (Fig. 6b) references

against the BBCEAS data. In Fig. 6a GLY show a good linearity from 5.4 to 48.2 ppbV and MGLY from 2.1 to 37.1 ppbV referenced to FTIR, respectively. In Fig. 6b, GLY show a good linearity from 1.0 to 33.3 ppbV and MGLY from 0.8 to 34.0 ppbV by BBCEAS, respectively. The linear equations for GLY between FTIR and BBCEAS are consistent in intercepts and gradients. Therefore, it can be concluded that there are no systematic differences among the calibrations equations established by the two independent reference techniques. Additionally, the correlation between FTIR and BBCEAS in GLY and MGLY determinations shown in Fig. 2b and c also confirms the good agreement in two reference techniques. Considering the BBCEAS technique has better accuracies and lower MDL than FTIR for both GLY and MGLY measurements, the calibration equations based on BBCEAS data are more preferable and used subsequently. The MDLs for the microfluidic method are estimated to be 80 pptV for GLY and 200 pptV for MGLY, which are calculated from the baseline signal plus 3 times standard deviation of the S/N of the blank sample in the GC chromatograph. Comparisons between the microfluidic derivatization technique and other previously reported methods for measuring GLY and MGLY, in term of linear range and detection limit are listed in Table 2. The detection limit of this technique is comparable with most spectrometric methods (Washenfelder et al., 2008; Thalman and Volkamer, 2010; Volkamer et al., 2005) and a little higher than the other derivatization methods (Lee and Zhou, 1993; Spaulding et al., 2002). However, the improved time resolution and automation are the significant advantages. Another method of calibration based on the measurement of standard solutions of α-dicarbonyl-PFBHA derivatives at different concentrations, is shown in Fig. 6c. The concentrations of α-dicarbonyl derivative solutions have been transformed into the mixing ratios of gaseous α-dicarbonyls assuming the derivatization efficiencies were 100 %. The gradients of the calibration equations based on standard solutions are higher than those based on BBCEAS data with 6.0 % and 7.5 % increases for MGLY and GLY, respectively, which may be caused by differences in reaction efficiencies for a derivatization reaction occurring in the micro-reactor instead of standard calibration solution. However, there are no systemic differences among the calibration equations established by

the standard calibration solutions and optical measurements, which implies the calibration solution method is feasible for gaseous GLY and MGLY determinations even if FTIR and BBCEAS are not available to provide independent reference measurements of the absolute gaseous α-dicarbonyl concentrations.

The average accuracies for GLY and MGLY are 6.6 % and 7.5 % which were calculated as the average relative error to the absolute concentrations provided by FTIR and BBCEAS, respectively. The precisions for GLY and MGLY are 11.2 % and 11.4 % respectively, which are the average Relative Standard Derivation (RSD) for the five parallel samples and five parallel injections. The detailed values for each measurement are shown in Table 3.

3.6   Application and direct comparisons with other techniques

To test the performance of the microfluidic derivatization technique for time resolved measurements, the technique was employed to determine gaseous GLY and MGLY during an experiment in the EUPHORE chamber to study the photo-oxidation of isoprene under relatively low NO_X ($NO \leq 2$ ppbV, NO_2 13–21 ppbV) conditions. The microfluidic technique was compared with FTIR, BBCEAS, PTR-ToF-MS and SPME derivatization techniques. The latest vision of the Master Chemical Mechanism (MCM v-3.2) was also employed in a chamber specific box model to predict the temporal evolution of the α-dicarbonyl products during the experiment. Comparisons of the five analytical techniques (focusing on the microfluidic derivatization technique) and the MCM box model simulation are shown in Fig. 7.

As shown in Fig. 7a, the microfluidic technique compares reasonably well with the FTIR measurement for both MGLY and GLY. The main inconsistencies shown are two higher concentration data points of MGLY (12.4 ± 3.9 and 7.4 ± 1.4 ppbV) measured by the microfluidic technique compared to those (6.90 ± 0.55 and 4.0 ± 0.30 ppbV) by the FTIR over the period of 240–280 min. GLY concentrations measured by the microfluidic technique are reasonably consistent with those detected by the FTIR over the entire experimental period. In comparison to BBCEAS technique (Fig. 7b), the concentra-

tions of MGLY and GLY measured by the microfluidic technique are also in reasonable agreement except for three higher data points around the same period as the FTIR inconsistencies occur (180–280 min). In this study the microfluidic technique and the SPME technique are both based on PFBHA derivatization. As Fig. 7c shows, the two techniques compared well (within their combined error bars) for GLY, which implies the PFBHA derivatization techniques are consistent and sufficiently sensitive to measure GLY in chamber applications. However, for MGLY measurement the two derivatization methods agree with each other during the initial stage of the experiment (up to 150 min), with MGLY concentrations measured by the microfluidic technique much higher than those by SPME after 150 min, which decrease much faster after this time. MGLY measured by PTR-ToF-MS also agrees reasonably well with those obtained by microfluidic derivatization technique during the initial rise up to about 200 min, as is shown in Fig. 7d. However, after this time the PTR-ToF-MS MGLY signal does not decay (whereas all other techniques do), but remains stable and constant for the remainder of the experiment. An explanation for this may be the background signal from the protonated water cluster $(H_2O)_4.H^+$ increases due to the increasing sample humidity and elevates background noise on the m/z 73 mass channel. As illustrated in Fig. 7e, the time-dependant trends of GLY and MGLY obtained by the detailed MCM box model agree reasonably well in term of profile shape and magnitude to those obtained by the microfluidic derivatization method, giving us some confidence in our understanding of the chemistry controlling isoprene photo-oxidation. However, the model tends to over-predict GLY and MGLY by a factor of approximate 1.3 and over-predicts GLY by a factor of 2.0 relative to the microfluidic technique before 180 min of the reaction, with agreement rather better during the second half, which may indicate some over prediction of the yields of secondary/tertiary products of isoprene oxidation (e.g. methacrolein/methyl vinyl ketone/glycolaldehyde), their α-dicarbonyls yields and/or under prediction of some α-dicarbonyl loss process(es) in the model.

To further test the feasibility of the microfluidic derivatization technique for measurements of GLY and MGLY at low concentrations, close to the detection limit, a com-

parison between microfluidic technique and BBCEAS data was conducted. As Fig. 8 shows, good agreements are observed for the measurements of GLY over the range of 0.1 ppbV to 0.8 ppbV and MGLY in the range of 0.9 ppbV to 1.7 ppbV. Some further refinement of the microfluidic technique will conducted to allow detection of ambient α-dicarbonyl measurements in the future principally through improvements in ruggedness and automation of the micro-reactor; the chamber experiments demonstrate however more than adequate sensitivity and time resolution.

From the smog chamber comparisons above it can be concluded that that microfluidic derivatization technique shows a similar performance, in terms of time profile shape and magnitude for GLY measurements as the SPME derivatization technique and the instrumental techniques of FTIR and BBCEAS. The microfluidic derivatization technique shows performance that better matches the reference FTIR and BBCEAS methods for MGLY than the SPME derivatization technique or PTR-ToF-MS.

4   Conclusions

A new, relatively sensitive and rapid automated microfluidic "lab-on-a-chip" derivatization technique has been developed for the sensitive measurement of gas-phase glyoxal (GLY) and methylglyoxal (MGLY) and been tested in a series of simulation experiments in EUPHORE chamber. The method is based on microfluidic derivatization of carbonyls and pre-concentration of the reaction solution in a glass micro-reactor followed by GC-MS analysis. The microchannels of the reactor enhance the phase contact area-to-volume ratio, and allow direct heating of the on-chip reaction. This combination of small volumes and higher temperatures creates a much faster and higher efficiency derivatization between α-dicarbonyls and PFBHA than can be achieved using other traditional derivatisation methods and without requiring any additional unwieldy preparative steps. Effluent leaving the micro-reactor can be directly injected into a standard benchtop GC-MS without further preparation. The technique was employed to measure the α-dicarbonyl products formed during a controlled isoprene photo-oxidation experiment

in the EUPHORE outdoor smog chamber, and was compared with several alternative spectroscopic and mass spectrometric techniques. The consistency in temporal evolutions of GLY and MGLY between different experimental measurement techniques and a detailed box model simulation provides some initial evidence for the effectiveness of the technique in practical applications. The microfluidic derivatization technique described provides significant opportunities to build on the specificity of derivatization for a series of carbonyls but at low cost, without manual preparative steps and allows for faster reaction times and on-line coupling with GC-MS.

References

Blake, R. S., Monks, P. S., and Ellis, A. M.: Proton-transfer reaction mass spectrometry, Chem. Rev., 109, 861–896, 2009. 5763

Bloss, C., Wagner, V., Bonzanini, A., Jenkin, M. E., Wirtz, K., Martin-Reviejo, M., and Pilling, M. J.: Evaluation of detailed aromatic mechanisms (MCMv3 and MCMv3.1) against environmental chamber data, Atmos. Chem. Phys., 5, 623–639, doi:10.5194/acp-5-623-2005, 2005. 5767

Calvert, J. G., Atkinson, R., Kerr, J., Madronich, S., Moortgat, G., Wallington, T., and Yarwood, G.: The Mechanisms of Atmospheric Oxidation of the Alkenes, vol. 5, Oxford University Press, New York, 2000. 5754, 5755, 5766

Calvert, J. G., Atkinson, R., Becker, K. H., Kamens, R. M., Seinfeld, J. H., Wallington, T. J., and Yarwood, G.: The Mechanisms of Atmospheric Oxidation of Aromatic Hydrocarbons, Oxford University Press, New York, 2002. 5754

Chan, A. W., Galloway, M. M., Kwan, A. J., Chhabra, P. S., Keutsch, F. N., Wennberg, P. O., Flagan, R. C., and Seinfeld, J. H.: Photooxidation of 2-methyl-3-buten-2-ol (MBO) as a potential source of secondary organic aerosol, Environ. Sci. Technol., 43, 4647–4652, 2009. 5755

Connelly, B., De Haan, D., and Tolbert, M.: Heterogeneous glyoxal oxidation: a potential source of secondary organic aerosol, J. Phys. Chem. A, 116, 6180–6187, 2012. 5756

De Haan, D. O., Corrigan, A. L., Tolbert, M. A., Jimenez, J. L., Wood, S. E., and Turley, J. J.: Secondary organic aerosol formation by self-reactions of methylglyoxal and glyoxal in evaporating droplets, Environ. Sci. Technol., 43, 8184–8190, 2009. 5754

Feierabend, K. J., Flad, J. E., Brown, S., and Burkholder, J. B.: HCO quantum yields in the photolysis of HC(O)C(O)H (glyoxal) between 290 and 420 nm, J. Phys. Chem. A, 113, 7784–7794, 2009. 5763

Finlayson-Pitts, B. J. and Pitts Jr., J. N.: Chemistry of the Upper and Lower Atmosphere: Theory, Experiments, and Applications, Academic Press, 1999. 5757

Fu, T.-M., Jacob, D. J., Wittrock, F., Burrows, J. P., Vrekoussis, M., and Henze, D. K.: Global budgets of atmospheric glyoxal and methylglyoxal, and implications for formation of secondary organic aerosols, J. Geophys. Res.-Atmos., 113, D15303, doi10.1029/2007JD009505, 2008. 5754, 5755

Galloway, M. M., Huisman, A. J., Yee, L. D., Chan, A. W. H., Loza, C. L., Seinfeld, J. H., and Keutsch, F. N.: Yields of oxidized volatile organic compounds during the OH radical initiated oxidation of isoprene, methyl vinyl ketone, and methacrolein under high-NO_x conditions, Atmos. Chem. Phys., 11, 10779–10790, doi:10.5194/acp-11-10779-2011, 2011. 5755

Gomez Alvarez, E., Borras, E., Viidanoja, J., and Hjorth, J.: Unsaturated dicarbonyl products from the OH-initiated photo-oxidation of furan, 2-methylfuran and 3-methylfuran, Atmos. Environ., 43, 1603–1612, 2009. 5758, 5762

Guenther A., Hewitt C., Erickson D., Fall, R., Geron, C., Graedel, T., Harley, P., Klinger, L., Lerdau, M., Mckay, W. A., Pierce, T., Scholes, B., Steinbrecher, R., Tallamraju, R., Taylor, J., and Zimmerman, P.: A global model of natural volatile organic compound emissions, J. Geophys. Res., 100, 8873–8892, 1995. 5755

Gurnick, M., Chaiken J., Benson, T., and McDonald, J.: Vibrational and rotational spectroscopy of the first electronically allowed transition of α-dicarbonyls, J. Chem. Phys. 74, 7 pp., doi10.1063/1.440800, 1981. 5764

Hallquist, M., Wenger, J. C., Baltensperger, U., Rudich, Y., Simpson, D., Claeys, M., Dommen, J., Donahue, N. M., George, C., Goldstein, A. H., Hamilton, J. F., Herrmann, H., Hoff-

A microfluidic measurement of glyoxal and methylglyoxal

X. Pang et al.

mann, T., Iinuma, Y., Jang, M., Jenkin, M. E., Jimenez, J. L., Kiendler-Scharr, A., Maenhaut, W., McFiggans, G., Mentel, Th. F., Monod, A., Prévôt, A. S. H., Seinfeld, J. H., Surratt, J. D., Szmigielski, R., and Wildt, J.: The formation, properties and impact of secondary organic aerosol: current and emerging issues, Atmos. Chem. Phys., 9, 5155–5236, doi:10.5194/acp-9-5155-2009, 2009. 5754

Heland, J., Kleffmann, J., Kurtenbach, R., and Wiesen, P.: A new instrument to measure gaseous nitrous acid (HONO) in the atmosphere, Environ. Sci. Technol., 35, 3207–3212, 2001. 5766

Henry, S. B., Kammrath, A., and Keutsch, F. N.: Quantification of gas-phase glyoxal and methylglyoxal via the Laser-Induced Phosphorescence of (methyl)GLyOxal Spectrometry (LIPG-LOS) Method, Atmos. Meas. Tech., 5, 181–192, doi:10.5194/amt-5-181-2012, 2012. 5754, 5755, 5756

Ho, S. S. H. and Yu, J. Z.: Feasibility of collection and analysis of airborne carbonyls by on-sorbent derivatization and thermal desorption, Anal. Chem., 74, 1232–1240, 2002. 5757, 5767, 5770, 5771

Ho, S. S. H. and Yu, J. Z.: Determination of airborne carbonyls: comparison of a thermal desorption/GC method with the standard DNPH/HPLC method, Environ. Sci. Technol., 38, 862–870, 2004. 5757

Hoffmann, T., Odum, J. R., Bowman, F., Collins, D., Klockow, D., Flagan, R. C., and Seinfeld, J. H.: Formation of organic aerosols from the oxidation of biogenic hydrocarbons, J. Atmos. Chem., 26, 189–222, 1997. 5754

Huisman, A. J., Hottle, J. R., Coens, K. L., DiGangi, J. P., Galloway, M. M., Kammrath, A., and Keutsch, F. N.: Laser-induced phosphorescence for the in situ detection of glyoxal at part per trillion mixing ratios, Anal. Chem., 80, 5884–5891, 2008. 5754, 5756, 5785

Huisman, A. J., Hottle, J. R., Galloway, M. M., DiGangi, J. P., Coens, K. L., Choi, W., Faloona, I. C., Gilman, J. B., Kuster, W. C., de Gouw, J., Bouvier-Brown, N. C., Goldstein, A. H., LaFranchi, B. W., Cohen, R. C., Wolfe, G. M., Thornton, J. A., Docherty, K. S., Farmer, D. K., Cubison, M. J., Jimenez, J. L., Mao, J., Brune, W. H., and Keutsch, F. N.: Photochemical modeling of glyoxal at a rural site: observations and analysis from BEARPEX 2007, Atmos. Chem. Phys., 11, 8883–8897, doi:10.5194/acp-11-8883-2011, 2011. 5756

Jenkin, M. E., Saunders, S. M., Wagner, V., and Pilling, M. J.: Protocol for the development of the Master Chemical Mechanism, MCM v3 (Part B): tropospheric degradation of aromatic

volatile organic compounds, Atmos. Chem. Phys., 3, 181–193, doi:10.5194/acp-3-181-2003, 2003. 5755, 5767

Langridge, J. M., Ball, S. M., Shillings, A. J., and Jones, R. L.: A broadband absorption spectrometer using light emitting diodes for ultrasensitive, in situ trace gas detection, Rev. Sci. Instrum., 79, 123110, 14 pp., doi:10.1063/1.3046282, 2008. 5756, 5762

Lee, Y. N. and Zhou, X.: Method for the determination of some soluble atmospheric carbonyl compounds, Environ. Sci. Technol., 27, 749–756, 1993. 5773

Lee, Y.-N., Zhou, X., and Hallock, K.: Atmospheric carbonyl compounds at a rural southeastern United States site, J. Geophys. Res., 100, 25933–25, 1995. 5754

Lee, Y.-N., Zhou, X., Kleinman, L. I., Nunnermacker, L. J., Springston, S. R., Daum, P. H., Newman, L., Keigley, W. G., Holdren, M. W., Spicer, C. W., Young, V., Fu, B., Parrish, D. D., Holloway, J., Williams, J., Roberts, J. M., Ryerson, T. B., and Fehsenfeld, F. C.: Atmospheric chemistry and distribution of formaldehyde and several multioxygenated carbonyl compounds during the 1995 Nashville/Middle Tennessee Ozone Study, J. Geophys. Res.-Atmos., 103, 22449–22462, 1998. 5757

Loeffler, K. W., Koehler, C. A., Paul, N. M., and De Haan, D. O.: Oligomer formation in evaporating aqueous glyoxal and methyl glyoxal solutions, Environ. Sci. Technol., 40, 6318–6323, 2006. 5754

MacDonald, S. M., Oetjen, H., Mahajan, A. S., Whalley, L. K., Edwards, P. M., Heard, D. E., Jones, C. E., and Plane, J. M. C.: DOAS measurements of formaldehyde and glyoxal above a south-east Asian tropical rainforest, Atmos. Chem. Phys., 12, 5949–5962, doi:10.5194/acp-12-5949-2012, 2012. 5754, 5756

Magneron, I., Mellouki, A., Le Bras, G., Moortgat, G., Horowitz, A., and Wirtz, K.: Photolysis and OH-initiated oxidation of glycolaldehyde under atmospheric conditions, J. Phys. Chem. A, 109, 4552–4561, 2005. 5755

Mauderly, J. L. and Chow, J. C.: Health effects of organic aerosols, Inhal. Toxicol., 20, 257–288, 2008. 5754

Munch, J., Munch, D., Winslow, S., Wendelken, S., and Pepich, B.: Determination of Carbonyl Compounds in Drinking Water by Pentafluorobenzyl Hydroxylamine Derivatization and Capillary Gas Chromatography with Electron Capture Detection, US EPA method, 556 pp., 1998. 5770

Munger, J. W., Jacob, D., Daube, B., Horowitz, L., Keene, W., and Heikes, B.: Formaldehyde, glyoxal, and methylglyoxal in air and cloudwater at a rural mountain site in central Virginia, J. Geophys. Res.-Atmos., 100, 9325–9333, 1995. 5754

Pang, X. and Lewis, A. C.: Carbonyl compounds in gas and particle phases of mainstream cigarette smoke, Sci. Total. Environ., 409, 5000–5009, 2011. 5757

Pang, X. and Lewis, A. C.: A microfluidic lab-on-chip derivatisation technique for the measurement of gas phase formaldehyde, Analytical Methods, 4, 2013–2020, 2012. 5759, 5760, 5765, 5767, 5771

Pang, X., Lewis, A. C., and Hamilton, J. F.: Determination of airborne carbonyls via pentafluorophenylhydrazine derivatisation by GC–MS and its comparison with HPLC method, Talanta, 85, 406–414, 2011. 5757

Profeta, L. T., Sams, R. L., Johnson, T. J., and Williams, S. D.: Quantitative infrared intensity studies of vapor-phase glyoxal, methylglyoxal, and 2,3-butanedione (diacetyl) with vibrational assignments, J. Phys. Chem. A, 115, 9886–9900, 2011. 5756

Reisen, F., Aschmann, S. M., Atkinson, R., and Arey, J.: Hydroxyaldehyde products from hydroxyl radical reactions of Z-3-hexen-1-ol and 2-methyl-3-buten-2-ol quantified by SPME and API-MS, Environ. Sci. Technol., 37, 4664–4671, 2003. 5771

Rickard, A., Wyche, K., Metzger, A., Monks, P., Ellis, A., Dommen, J., Baltensperger, U., Jenkin, M., and Pilling, M.: Gas phase precursors to anthropogenic secondary organic aerosol: using the master chemical mechanism to probe detailed observations of 1, 3, 5-trimethylbenzene photo-oxidation, Atmos. Environ., 44, 5423–5433, 2010. 5767

Sinreich, R., Coburn, S., Dix, B., and Volkamer, R.: Ship-based detection of glyoxal over the remote tropical Pacific Ocean, Atmos. Chem. Phys., 10, 11359–11371, doi:10.5194/acp-10-11359-2010, 2010. 5754

Solomon, S.: Climate Change 2007 – The Physical Science Basis: Working Group I Contribution to the Fourth Assessment Report of the IPCC, Vol. 4, Cambridge University Press, 2007. 5754

Spaulding, R. S., Talbot, R. W., and Charles, M. J.: Optimization of a mist chamber (cofer scrubber) for sampling water-soluble organics in air, Environ. Sci. Technol., 36, 1798–1808, 2002. 5767, 5773, 5785

Spaulding, R. S., Schade, G. W., Goldstein, A. H., and Charles, M. J.: Characterization of secondary atmospheric photooxidation products: evidence for biogenic and anthropogenic sources, J. Geophys. Res., 108, 4247, doi:10.1029/2002JD002478, 2003. 5754

Title Page

Abstract | Introduction

Conclusions | References

Tables | Figures

|◄ | ►|

◄ | ►

Back | Close

Full Screen / Esc

Printer-friendly Version

Interactive Discussion

Temime, B., Healy, R. M., and Wenger, J. C.: A denuder-filter sampling technique for the detection of gas and particle phase carbonyl compounds, Environ. Sci. Technol., 41, 6514–6520, 2007. 5757, 5769, 5770, 5771

Thalman, R. and Volkamer, R.: Inherent calibration of a blue LED-CE-DOAS instrument to measure iodine oxide, glyoxal, methyl glyoxal, nitrogen dioxide, water vapour and aerosol extinction in open cavity mode, Atmos. Meas. Tech., 3, 1797–1814, doi:10.5194/amt-3-1797-2010, 2010. 5756, 5773, 5785

Tuazon, E. C., Atkinson, R., Mac Leod, H., Biermann, H. W., Winer, A. M., Carter, W. P., and Pitts, J. N.: Yields of glyoxal and methylglyoxal from the nitrogen oxide (NO_x)-air photooxidations of toluene and m- and p-xylene, Environ. Sci. Technol., 18, 981–984, 1984. 5755

Volkamer, R., Molina, L. T., Molina, M. J., Shirley, T., and Brune, W. H.: DOAS measurement of glyoxal as an indicator for fast VOC chemistry in urban air, Geophys. Res. Lett., 32, L08806, doi:10.1029/2005GL022616, 2005. 5754, 5755, 5756, 5773, 5785

Volkamer, R., San Martini, F., Molina, L. T., Salcedo, D., Jimenez, J. L., and Molina, M. J.: A missing sink for gas-phase glyoxal in Mexico City: formation of secondary organic aerosol, Geophys. Res. Lett., 34, L19807, doi:10.1029/2007GL030752, 2007. 5754, 5755

Volkamer, R., Ziemann, P. J., and Molina, M. J.: Secondary Organic Aerosol Formation from Acetylene (C_2H_2): seed effect on SOA yields due to organic photochemistry in the aerosol aqueous phase, Atmos. Chem. Phys., 9, 1907–1928, doi:10.5194/acp-9-1907-2009, 2009. 5754

Vrekoussis, M., Wittrock, F., Richter, A., and Burrows, J. P.: Temporal and spatial variability of glyoxal as observed from space, Atmos. Chem. Phys., 9, 4485–4504, doi:10.5194/acp-9-4485-2009, 2009. 5754, 5757

Vrekoussis, M., Wittrock, F., Richter, A., and Burrows, J. P.: GOME-2 observations of oxygenated VOCs: what can we learn from the ratio glyoxal to formaldehyde on a global scale?, Atmos. Chem. Phys., 10, 10145–10160, doi:10.5194/acp-10-10145-2010, 2010. 5757

Washenfelder, R. A., Langford, A. O., Fuchs, H., and Brown, S. S.: Measurement of glyoxal using an incoherent broadband cavity enhanced absorption spectrometer, Atmos. Chem. Phys., 8, 7779–7793, doi:10.5194/acp-8-7779-2008, 2008. 5756, 5773, 5785

Washenfelder, R. A., Young, C. J., Brown, S. S., Angevine, W. M., Atlas, E. L., Blake, D. R., Bon, D. M., Cubison, M. J., de Gouw, J. A., Dusanter, S., Flynn, J., Gilman, J. B., Graus, M., Griffith, S., Grossberg, N., Hayes, P. L., Jimenez, J. L., Kuster, W. C., Lefer, B. L., Pollack, I. B., Ryerson, T. B., Stark, H., Stevens, P. S., and Trainer, M. K.: The glyoxal budget and its

Title Page

Abstract | Introduction

Conclusions | References

Tables | Figures

◄ | ►|

◄ | ►

Back | Close

Full Screen / Esc

Printer-friendly Version

Interactive Discussion

contribution to organic aerosol for Los Angeles, California, during CalNex 2010, J. Geophys. Res.-Atmos., 116, D00V02, doi10.1029/2011JD016314, 2011. 5756

Wittrock, F., Richter, A., Oetjen, H., Burrows, J. P., Kanakidou, M., Myriokefalitakis, S., Volkamer, R., Beirle, S., Platt, U., and Wagner, T.: Simultaneous global observations of glyoxal and formaldehyde from space, Geophys. Res. Lett., 33, L16804, doi:10.1029/2006GL026310, 2006. 5757

Yu, J., Jeffries, H. E., and Le Lacheur, R. M.: Identifying airborne carbonyl compounds in isoprene atmospheric photooxidation products by their PFBHA oximes using gas chromatography/ion trap mass spectrometry, Environ. Sci. Technol., 29, 1923–1932, 1995. 5768

Title Page

Abstract | Introduction

Conclusions | References

Tables | Figures

|◄ | ►|

◄ | ►

Back | Close

Full Screen / Esc

Printer-friendly Version

Interactive Discussion

5783

Table 1. Optimal experimental conditions for the microfluidic derivatization reaction between PFBHA and gaseous α-dicarbonyls in the micro-reactor.

PFBHA concentration	Temperature (°C)	Flow rate of α-dicarbonyls (mL min^{-1})	Flow rate of solution (µL min^{-1})
5×10^{-4} mol L^{-1}	60	200	40

Table 2. Comparison between microfluidic derivatization technique and other methods in linear range and method detection limit (MLD).

Analytical technique	GLY		MGLY		Ref
	Linear range (ppbV)	MLD[a] (ppbV)	Linear range (ppbV)	MLD (ppbV)	
Microfluidic	0.7–400	0.08	1.2–300	0.2	This study
FTIR	2.5–3500	2.5	2.7–4200	2.7	This study
SPME	1–130	0.1	1–80	0.15	This study
PTR-ToF-MS	–[b]	–	1.7–172	1.5	This study
BBCEAS	0.05–300	0.07	0.4–400	1.0	This study
Mad LIP	–	0.02	–	–	(Huisman et al., 2008)
IBBCEAS	–	0.13	–	–	(Washenfelder et al., 2008)
LED-CE-DOAS	–	0.03	–	0.255	(Thalman and Volkamer, 2010)
DOAS	–	0.15	–	–	(Volkamer et al., 2005)
PFBHA-mist chamber	–	0.003	–	0.01	(Spaulding et al., 2002)

[a] MLDs are 3 times standard deviation of the S/N of the blank sample chromatrograph.

[b] No data available.

Table 3. Accuracy and precision of the microfluidic derivatization technique.

Absolute concn. (ppbV)[a]		Observed concn. (ppbV)[b]		Accuracy (%)[c]		Precision of reactor (%)[d]		Precision of GC-MS (%)[e]		Total precision (%)[f]	
GLY	MGLY	GLY	MGLY	GLY	MGLY	GLY	MGLY	GLY	MGLY	GLY	MGLY
40.2	121.3	37.5	115.6	6.7	7.7	7.6	7.4	3.5	3.8	11.1	11.2
29.5	85.0	28.3	81.5	6.3	7.1	7.5	6.9	3.4	3.9	10.9	11.1
19.4	56.3	18.1	53.6	6.7	7.8	6.5	6.8	5.9	5.1	11.7	11.9

[a] Absolute concentrations of GLY and MGLY were given by BBCEAS.
[b] Observed concentrations were measured by microfluidic derivatization technique.
[c] Accuracy of the method was calculated by [(observed concentration-absolute concentration)/absolute concentration] × 100 %.)
[d] RSD (Relative Standard Deviation) of replicate analyses ($n = 5$) of standard a-dicarbonyl gases.
[e] RSD of repeated measurements ($n = 5$) under the same GC-MS conditions. RSD = [(standard deviation of observed concentration)/(average of observed concentration)] × 100 %.
[f] Sum of precision of reactor and GC-MS.

Fig. 1. (a) Basic layout of micro-reactor including three inputs, one output, mixing junctions, and 208 cm reacting microchannel (size: length × width × thickness = 90 mm × 45 mm × 4.5 mm). **(b)** Schematics of the microfluidic lab-on-chip derivatization system. Derivative solution was collected directly from micro-reactor and ready to GC-MS analysis.

Title Page

Abstract | Introduction

Conclusions | References

Tables | Figures

◀ | ▶

◀ | ▶

Back | Close

Full Screen / Esc

Printer-friendly Version

Interactive Discussion
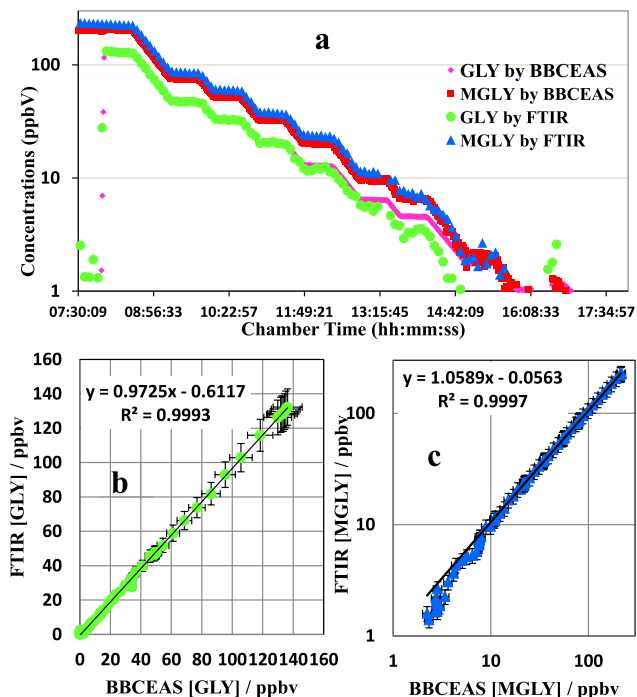
Fig. 2. Comparison between FTIR and BBCEAS measurements of GLY and MGLY. **(a)** Comparison between FTIR and BBCEAS measurements during preparation of standard gaseous GLY and MGLY mixture in the EUPHORE chamber; **(b)** linear relationship between FTIR and BBCEAS on GLY measurement (error bars indicate the accuracies of FTIR and BBCEAS on GLY measurement); **(c)** linear relationship between FTIR and BBCEAS on MGLY measurement (error bars indicate the accuracies of FTIR and BBCEAS on MGLY measurement).
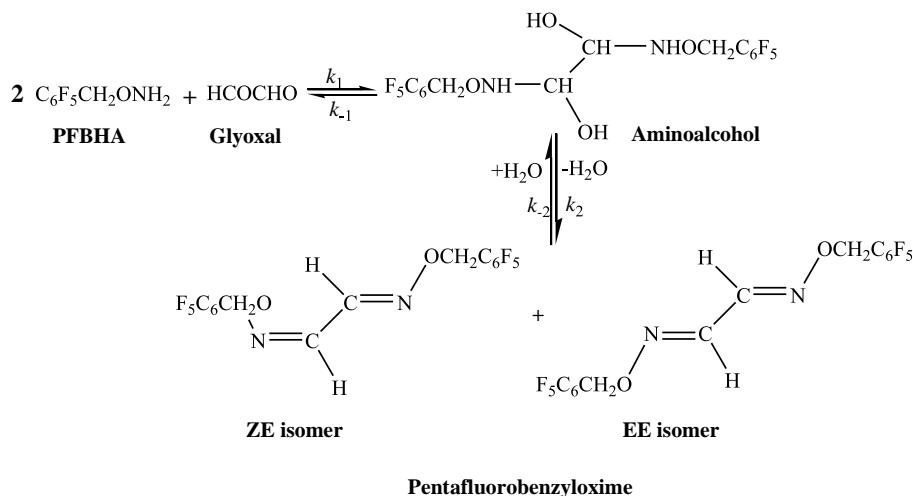
Fig. 3. Two-step process of derivatization of GLY with PFBHA to form the corresponding derivative oxime isomers.
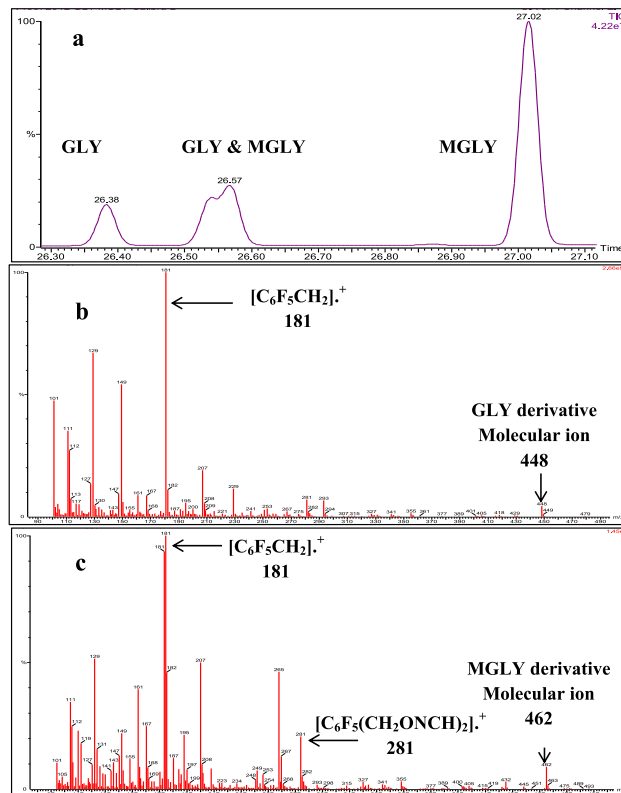
Fig. 4. GC-MS chromatogram (**a**) of PFBHA derivatives of GLY and MGLY and their EI mass spectra (**b** for GLY at 26.38 min and **c** for MGLY at 27.02 min). Fragmentation m/z 181 Da, the most abundant ion, is chosen for Selective Ion Monitoring (SIM) to quantify the derivative concentrations and to obtain best sensitivity. Only the GC peak of GLY derivative at retention time of 26.38 min and the GC peak of MGLY derivative at retention time of 27.0 min were used to quantify derivative concentration of each individual α-dicarbonyl.
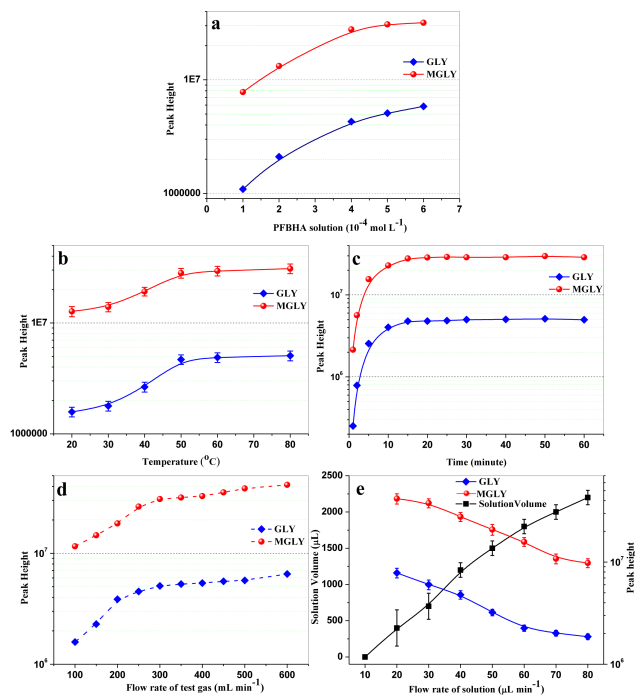
Fig. 5. Influences of PFBHA concentration (**a**), temperature of micro-reactor (**b**), reaction time (**c**), flow rates of GLY and MGLY gas (**d**) and flow rate of derivatization solution (**e**) on the peak heights of derivatives in GC-MS chromatograms. Error bars indicate the relative standard deviation of GC measurements.
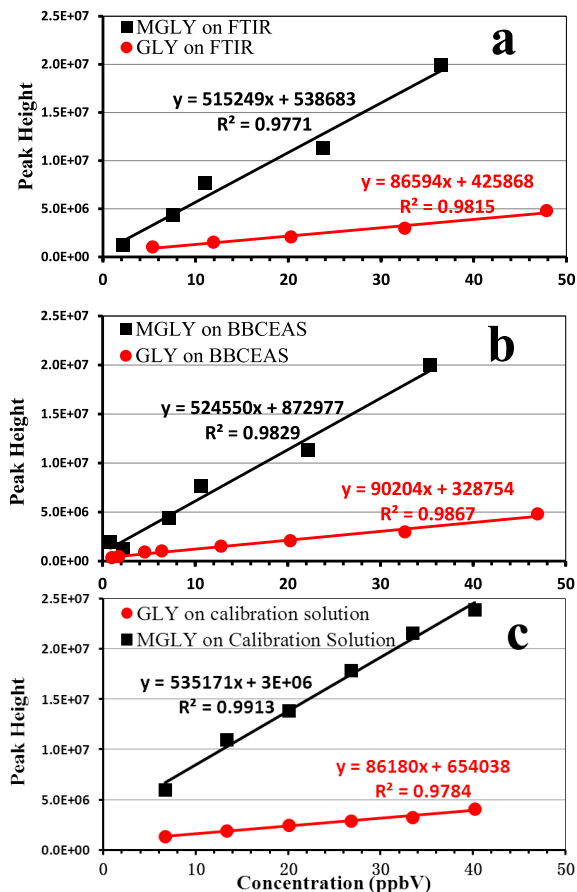
Fig. 6. Calibration curves of GLY and MGLY based on the absolute α-dicarbonyl data provided by FTIR (**a**) and by BBCEAS (**b**) measured by the microfluidic derivatization technique under the optimal conditions. Calibration curves of GLY and MGLY in (**c**) are established by the calibration solution of α-dicarbonyl derivatives.

Title Page

Abstract | Introduction

Conclusions | References

Tables | Figures

◄ | ►◄

◄ | ►

Back | Close

Full Screen / Esc

Printer-friendly Version

Interactive Discussion
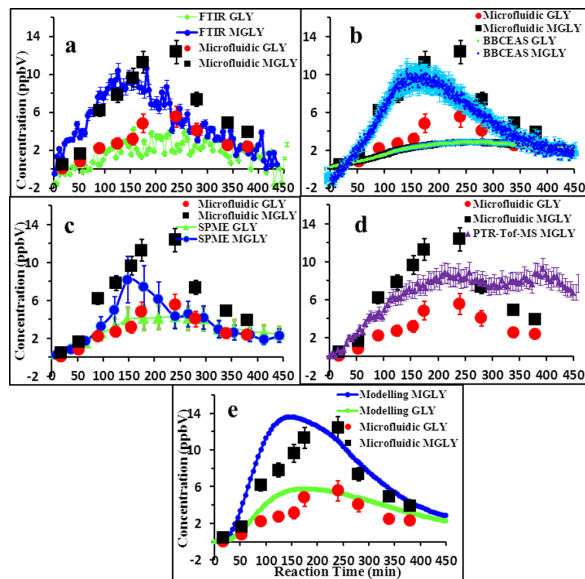
Fig. 7. Comparison of the microfluidic derivatization technique, FTIR, BBCEAS, PTR-ToF-MS, SPME derivatization technique and a MCM (v3.2) box model simulation on gaseous GLY and MGLY measurements during isoprene photo-oxidation in EUPHORE chamber. **(a)** Comparison microfluidic derivatization with FTIR; error bars on the FTIR data represent an 8 % of accuracy for α-dicarbonyls measurements and error bars on microfluidic derivatization data represent the 6.7 % of accuracy for GLY and 8 % of accuracy for MGLY measurement; **(b)** comparison microfluidic derivatization with the BBCEAS technique; error bars on BBCEAS data indicate represent a 7 % of accuracy for GLY quantification and a 10 % of accuracy for MGLY quantification by BBCEAS. **(c)** Comparison with SPME derivatization techniques, error bars for SPME are the 30 % of accuracies for both α-dicarbonyl quantifications; **(d)** comparison microfluidic derivatization with PTR-ToF-MS, error bars for PTR-ToF-MS are the 13 % of accuracy for MGLY quantification; **(e)** comparison microfluidic derivatization with MCM modelling prediction.

Fig. 8. Intercomparison of microfluidic dirivatization technique and BBCEAS on measurements of GLY and MGLY at low concentrations near detection limits. **(a)** Linear relationship between microfluidic derivatization and BBCEAS for GLY measurement (error bars indicate the accuracies of microfluidic derivatization and BBCEAS for GLY measurement); **(b)** linear relationship between microfluidic derivatization and BBCEAS for MGLY measurement (error bars indicate the accuracies of FTIR and BBCEAS for MGLY measurement).